BMC Oral Health

RESEARCH Open Access

Differentially expressed extracellular matrix genes functionally separate ameloblastoma from odontogenic keratocyst

Prasath Jeyaraman[1], Arularasan Anbinselvam[1] and Sunday O. Akintoye[1*]

Abstract

Background Ameloblastoma and odontogenic keratocyst (OKC) are odontogenic tumors that develop from remnants of odontogenic epithelium. Both display locally invasive growth characteristics and high predilection for recurrence after surgical removal. Most ameloblastomas harbor BRAFV600E mutation while OKCs are associated with PATCH1 gene mutation but distinctive indicators of ameloblastoma growth characteristics relative to OKC are still unclear. The aim of this study was to assess hub genes that underlie ameloblastoma growth characteristics using bioinformatic analysis, ameloblastoma samples and mouse xenografts of human epithelial-derived ameloblastoma cells.

Methods RNA expression profiles were extracted from GSE186489 gene expression dataset acquired from Gene Expression Ominibus (GEO) database. Galaxy and iDEP online analysis tools were used to identify differentially expressed genes that were further characterized by gene ontology (GO) and pathway analysis using ShineyGO. The protein-protein interaction (PPI) network was constructed for significantly upregulated differentially expressed genes using online database STRING. The PPI network visualization was performed using Cytoscape and hub gene identification with cytoHubba. Top ten nodes were selected using maximum neighborhood component, degree and closeness algorithms and analysis of overlap was performed to confirm the hub genes. Epithelial-derived ameloblastoma cells from conventional ameloblastoma were transplanted into immunocompromised mice to recreate ameloblastoma in vivo based on the mouse xenograft model. The top 3 hub genes FN1, COL I and IGF-1 were validated by immunostaining and quantitative analysis of staining intensities to ameloblastoma, OKC samples and mouse ameloblastoma xenografts tissues.

Results Seven hub genes were identified among which FN1, COL1A1/COL1A2 and IGF-1 are associated with extracellular matrix organization, collagen binding, cell adhesion and cell surface interaction. These were further validated by positive immunoreactivity within the stroma of ameloblastoma samples but both ameloblastoma xenograft and OKC displayed only FN1 and IGF-1 immunoreactivity while COL 1 was unreactive. The expression levels of both FN1 and IGF-1 were much lower in OKC relative to ameloblastoma.

*Correspondence:
Sunday O. Akintoye
akintoye@upenn.edu

Full list of author information is available at the end of the article

Conclusion This study further validates a differentially upregulated expression of matrix proteins FN1, COL I and IGF-1 in ameloblastoma relative to OKC. It suggests that differential stromal architecture and growth characteristics of ameloblastoma relative to OKC could be an interplay of differentially upregulated genes in ameloblastoma.

Keywords Ameloblastoma, Gene expression, Invasive growth, Odontogenic keratocyst, Extracellular matrix

Introduction

Ameloblastoma is a highly recurrent odontogenic tumor of epithelial origin [1]. Incidence rate of ameloblastoma is about 0.5 to 1 per million people per year making it a relatively rare and understudied disease [2, 3]. Recent advances on the genetics of ameloblastoma have provided more insights on ameloblastoma growth characteristics, clinico-pathological correlations, maxillo-mandibular site distribution within the jaws and microenvironmental factors that promote ameloblastoma recurrence [4–7]. The 2022 World Health Organization (WHO) classification of odontogenic tumors now includes adenoid ameloblastoma as part of benign ameloblastomas in addition to conventional, unicystic, extraosseous/peripheral and metastasizing ameloblastomas while ameloblastic carcinoma is still the lone malignant type [8, 9]. About 80% of ameloblastomas harbor mutations in the mitogen-activated protein kinase (MAPK)-related B-raf proto-oncogene (BRAF) [1] and a smaller subset display mutation of smoothened (SMO), a G protein-coupled receptor and signaling effector component of hedgehog (Hh) signaling pathway [1, 4, 10]. Considering that MAPK and Hedgehog signalling pathways are actively involved in tooth development in both the maxilla and mandible, it is intriguing that BRAF mutation is more common in mandibular ameloblastoma while KRAS, FGFR2 and SMO mutations are more common in maxillary ameloblastomas [4]. Remnants of the dental epithelium persists as epithelial residues long after tooth development and eruption into the oral cavity. While these epithelial remnants normally remain quiescent and inactive, it is believed that their reactivation can be associated with development of several inflammatory, cystic, and neoplastic lesions in the jaw such as ameloblastoma and odontogenic keratocyst (OKC) [11].

Histologically, ameloblastoma resembles the enamel organ of a developing tooth with a stroma devoid of dental mesenchyme [1]. Most ameloblastoma lesions are benign, but they exhibit locally aggressive growth characteristics and high recurrence rate [1]. Like ameloblastoma, OKC is a cystic jaw lesion that arises from odontogenic epithelium, demonstrates locally aggressive growth and high recurrence potential but its molecular signature is associated with PATCH1 gene mutation [12]. PATCH1 inhibits Hh signalling pathway by repressing activity of SMO. Compared to ameloblastoma, SMO mutation in OKC is rare, but both share the effects of a dysregulated Hh signalling. Contrarywise, BRAF mutation is well established in ameloblastoma but reports on etiological association of BRAF mutation with OKC are still unclear and conflicting [13–15]. Although both ameloblastoma and OKC develop from odontogenic epithelial remnants, a comparison of their gene expression profiles showed that early dental epithelium markers were differentially upregulated in ameloblastoma compared to upregulation of squamous epithelial differentiation markers in OKC [16]. So ameloblastoma reflects epithelial differentiation toward the enamel organ while OKC differentiation is in the direction of keratinocytes [16]. Hence, there are both similarities and differences in the pathophysiological and recurrence characteristics of ameloblastoma and OKC attributable to their molecular etiological differences. Ameloblastoma recurrence is attributable to post-surgical remnants of invasive odontogenic epithelium and OKC recurrence is associated with post-surgical daughter/satellite cysts that reactivate to promote recurrence [1]. Single cell transcriptomics and cell cycle analysis have also revealed that presence of high cycling ameloblastoma cells are associated with cell survival, self-renewal and tumor cell reactivation that result in ameloblastoma recurrence [17].

A clear understanding of the locally invasive growth characteristics of ameloblastoma is needed to enable the development of therapeutic targets. Ameloblastoma is a highly recurrent tumor and there are still no biological markers to predict which ameloblastoma will recur post-treatment. Therefore, the aim of this study was to assess biological indicators of aggressive growth properties of ameloblastoma relative to OKC using gene expression datasets, ameloblastoma and OKC tissue samples and xenografts derived from epithelial-derived ameloblastoma cells. Further insights into these biological markers have the potential to lead to therapeutic targets and predictors of post-treatment recurrence [5, 7, 18].

Materials and methods

RNA sequencing data collection

We downloaded the GSE186489 gene expression data from Gene Expression Omnibus (GEO) database (https://www.ncbi.nlm.nih.gov/geo/query/acc.cgi?acc=GSE186489), based on GPL16791 Illumina HiSeq 2500 (Homo sapiens) platform. The dataset includes gene expression data from three ameloblastoma and three odontogenic keratocyst (OKC) samples.

Identification of differentially expressed genes

The online data analysis platforms Galaxy and iDEP (integrated Differential Expression and Pathway analysis) [19] were used to analyze the gene dataset. From the Galaxy platform, FASTQ files were extracted using Sequence Read Archive (SRA) numbers for the dataset GSE186489. RNA STAR was used to align the sequence using reference genome (hg38) after checking the quality with FastQC. Gene counts were obtained using featureCounts and inputted into the iDEP platform for the differential gene expression analysis. Significant differentially expressed genes (DEGs) were identified by applying the cut off for p value (≤ 0.05) and |log2 fold change| ≥ 2 as previously described [20].

Gene ontology and pathway analysis

Differentially expressed genes (DEGs) were further characterized by gene ontology (GO) and pathway analysis using ShineyGO [21]. The false discovery rate (FDR) threshold was set to 0.05 and the GO terms were obtained for biological process (BP), cellular components (CC), molecular functions (MF) and pathway enrichment using Reactome [22].

Protein-protein interaction network and hub gene analysis

The Protein-Protein Interaction (PPI) network was constructed for significantly upregulated DEGs using online database STRING (version 12.0) (https://string-db.org/) with the confidence score of 0.9 to get the most significant interactions. Then, the PPI network visualization was performed using Cytoscape (version v3.10.1) and hub gene identification with the plugin cytoHubba [20]. The top 10 nodes were selected using three algorithms (Maximum Neighborhood Component (MNC), Degree and Closeness) and analysis of overlap was performed to confirm the hub genes.

Tissue processing

Ameloblastoma surgical samples ($n=13$) were used for validation of the top pathway genes identified. Ameloblastoma tissues were collected from patients enrolled in protocol 849,919 approved by University of Pennsylvania Office of Regulatory Affairs Institutional Review Board (IRB). Representative portions of the samples were fixed in 4% paraformaldehyde (PFA). Additionally, archival paraffin-embedded OKC tissue blocks ($n=2$, provided courtesy of Dr. Abdul-Warith Akinshipo, Lagos University Teaching Hospital, Lagos Nigeria) were used for comparative analysis. From both ameloblastoma and OKC, 5 µm sections were stained with hematoxylin-eosin for histological analysis while unstained sections were used for immunohistochemical analysis. Another representative portions of ameloblastoma patient samples were processed to establish primary epithelial-derived ameloblastoma cells (EPAMCs) as previously reported [7]. Two board-certified oral pathologists confirmed the diagnosis of the ameloblastoma samples based on current World Health Organization (WHO) classification of odontogenic tumors [8, 23].

Mouse xenograft model of ameloblastoma

Mouse in vivo tumor model was used to further assess biological function of the top gene interactions. Mouse model of ameloblastoma was based on patient-derived xenograft was used to recreate in vivo ameloblastoma. The animal protocol (# 806165) was approved by the University of Pennsylvania Institutional Animal Care and Use Committee. Described briefly here, the isolated and characterized EPAMCs from conventional ameloblastoma were revived and seeded in triplicate flasks [7]. Approximately 2×10^6 EPAMCs attached to 40 mg of spheroidal hydroxyapatite/tricalcium phosphate (HA/TCP, particle size 0.5–1.0 mm, Zimmer, Warsaw, IN) were transplanted into subcutaneous pockets of 4-week-old immunocompromised nude female mice (Charles River Laboratories, Wilmington, MA) as previously described [7]. Prior to EPAMC transplantation, animals were anesthetized with combination of medetomidine (0.5-1 mg/kg body weight) and ketamine (70–100 mg/kg body weight). A combination of lidocaine/bupivacaine (1:1 ratio) was used to anesthetize the surgical site to control peri-operative pain. All animal transplants were performed using triplicate animals and each animal received 3 to 4 grafts to minimize individual animal variability. At the conclusion of EPAMC transplantation, the effect of medetomidine was reversed with atipamezole (1 mg/kg body weight) and meloxicam-XR (6 mg/kg body weight) was used to control post-operative pain. At week 4, animals were euthanized with carbon dioxide delivered using euthanasia apparatus. Euthanasia was confirmed by cervical dislocation. The xenografts were harvested, fixed with 4% PFA in PBS (pH 7.4), decalcified in 10% EDTA (pH 8.0), embedded in paraffin and 5 µm sections were stained with hematoxylin/eosin (H&E) for histological evaluation.

Immunohistochemical assessment

Ameloblastoma, EPAMCs mouse xenografts and OKC tissues were processed for immunostaining using standard protocols. The tissue sections were deparaffinized in 100% xylene and rehydrated in series of graded ethanol followed by antigen retrieval at 95 °C for 20 min using Antigen Unmasking Solution, Citric Acid Based (H-3300, Vector Laboratories, Newark, CA. USA). Endogenous peroxidase was blocked with BLOXALL® Endogenous Blocking Solution (SP-6000, Vector Laboratories, Newark, CA. USA) for 10 min at room temperature. The sections were then blocked with normal blocking solution

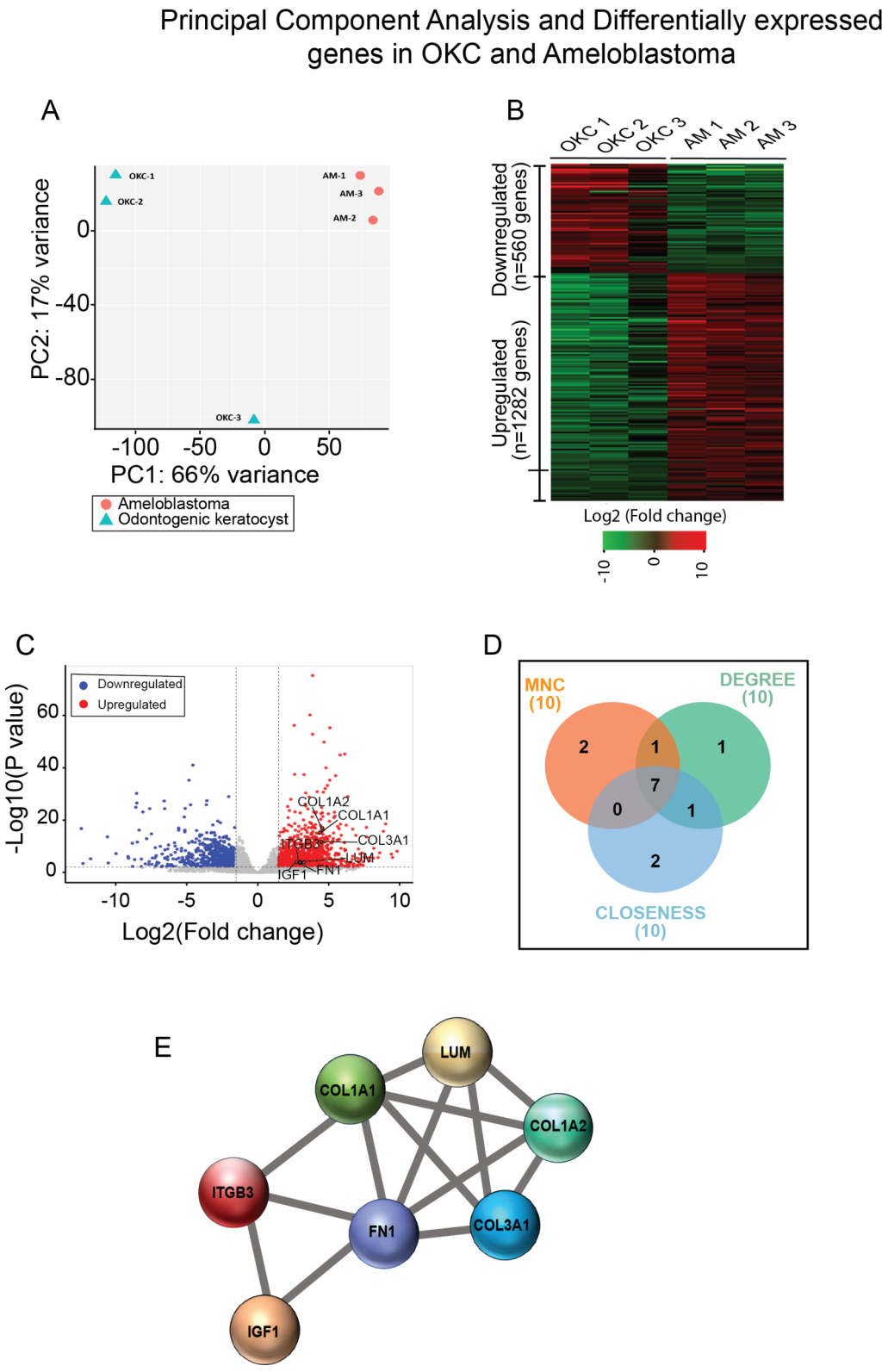

Fig. 1 (See legend on next page.)

(See figure on previous page.)

Fig. 1 Differential gene expression analysis and hub gene identification. (**A**) Principal component analysis shows the clear difference between three ameloblastoma (AM) and three odontogenic keratocyst (OKC) samples as well as the small variation between the OKC patients. (**B**) Heatmap of differentially expressed genes (DEGs) in ameloblastoma shows 560 downregulated and 1282 upregulated genes. (**C**) Volcano plot shows the DEGs in ameloblastoma with the major hub genes labelled. The significant DEGs ($p < 0.05$ and |log2 fold change|≥2) is indicated by the red (upregulated) and blue (downregulated) dots. A horizonal dashed line indicate $p \leq 0.05$ and vertical dashed lines mark fold change ≥ 2. (**D**) Seven hub genes were identified from the top 10 nodes of three cytohubba algorithms, Maximum Neighborhood Component (MNC), Degree and Closeness (**E**) Visualization of the PPI network of identified hub genes

(VECTASTAIN® Elite ABC-HRP Kit, PK-6200, Vector Laboratories, Newark, CA. USA) at room temperature for 1 h followed by incubation at 4 °C overnight with each of the following primary antibodies: Fibronectin (FN1) monoclonal antibody (1:300, Cat # 66042-1-Ig, Proteintech, Rosemont IL. USA), Collagen I (COL 1) antibody (1;500; Cat # ab138492, Abcam, Waltham, MA) and Insulin-like Growth Factor-1 (IGF-1) polyclonal antibody (1:50; Cat # bs-0014R, Bios Inc, Woburn, MA) and isotype control non-immune serum. Subsequently, tissue sections were rinsed with PBS before incubating at room temperature for 30 min with VECTASTAIN® biotinylated universal secondary antibody and ABC reagents (Vector Laboratories, Newark, CA). Finally, specimens were stained with DAB Substrate Kit (SK-4100, Vector Laboratories, Newark, CA) and counterstained with hematoxylin (26030-20, Electron Microscopy Sciences, Hatfield, PA). Microscopic evaluation of immunoreactivity and image capture was performed using Nikon Eclipse 80i (Nikon Instruments, Melville, NJ) equipped with SPOT Flex digital camera (Diagnostic Instruments, Sterling Heights, MI). The immunostaining image intensities were quantified using Image J (Fiji v2.0.0; National Institutes of Health, Bethesda, MD). and its color-deconvolution plugin to isolate the red, green and blue spectra of DAB images as previously described [24]. The brown DAB-stained images were converted to binary black and white images. Optical density of stained randomly selected four regions of interest (ROI) was calculated and normalized to its respective control tissues to obtain average mean intensity per unit area.

Results

Differential gene expression analysis and hub gene identification

Principal component analysis (PCA) plot of datasets of ameloblastoma and OKC patient samples illustrate differences between ameloblastoma and OKC. The ameloblastoma samples showed concordance by clustering together, but there was a minor variation among the OKC samples as one of the samples (OKC-3) did not cluster with the other two samples (Fig. 1A). Heatmap (Fig. 1B) and volcano plot (Fig. 1C) were used to visualize the significant DEGs between ameloblastoma and OKCs. The heatmap of 1842 DEGs showed there were 560 downregulated and 1282 upregulated genes in ameloblastoma relative to OKC (see Supplementary Table and Fig. 1B). Venn diagram was used to identify seven overlapping hub genes from the top 10 nodes of three cytohubba algorithms, Maximum Neighborhood Component (MNC), Degree and Closeness (Fig. 1D). The PPI network visualization is presented in Fig. 1E.

GO and pathway enrichment analysis

The top 10 enriched GO terms for biological process (BP) (Fig. 2A), cellular component (CC) (Fig. 2B), molecular function (MF) (Fig. 2C) and Reactome pathways (Fig. 2D) were identified by GO enrichment and Reactome

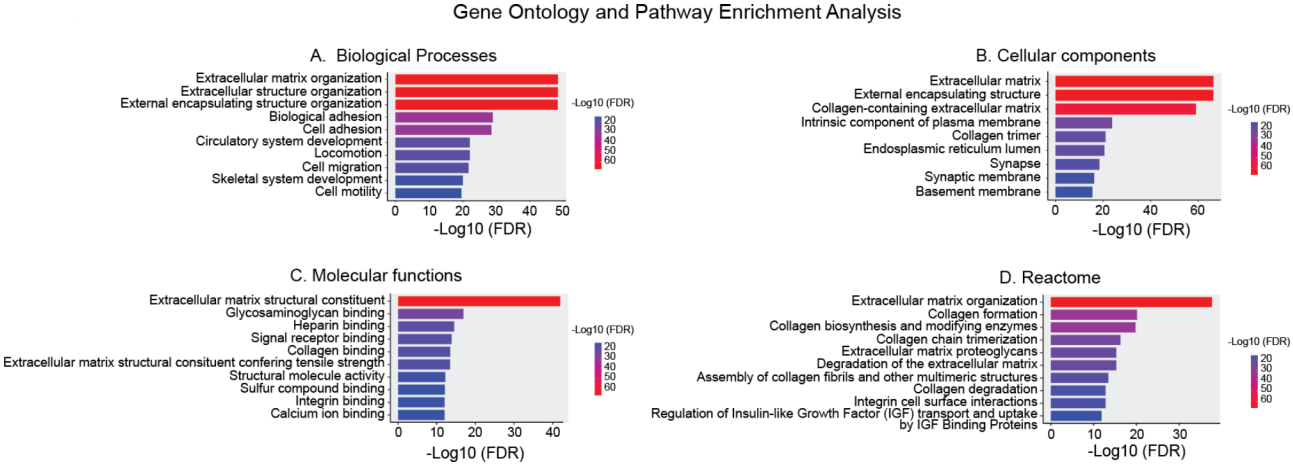

Fig. 2 Gene ontology and pathway enrichment analysis. The bar graphs display the Top 10 enriched gene ontology terms for biological process (**A**), cellular components (**B**), molecular functions (**C**) and the Top 10 enriched Reactome pathways (**D**)

Table 1 Identification of top 10 hub genes by three cytoHubba algorithms

Maximum Neighborhood Component (MNC) Algorithm	
FN1	Fibronectin 1
COL1A1	Collagen type I alpha 1 chain
COL1A2	Collagen type I alpha 2 chain
LUM	Lumican
COL3A1	Collagen type III alpha 1 chain
ITGB3	Integrin subunit beta 3
ACAN	Aggrecan
IGF1	Insulin like growth factor 1
COL5A2	Collagen type V alpha 2 chain
MMP9	Matrix metallopeptidase 9
Degree Algorithm	
FN1	Fibronectin 1
COL1A2	Collagen type I alpha 2 chain
COL1A1	Collagen type I alpha 1 chain
FBN1	Fibrillin 1
LUM	Lumican
COL3A1	Collagen type III alpha 1 chain
ITGB3	Integrin subunit beta 3
ACAN	Aggrecan
ENPP1	Ectonucleotide pyrophosphatase/phosphodiesterase 1
IGF1	Insulin like growth factor 1
Closeness Algorithm	
FN1	Fibronectin 1
ITGB3	Integrin subunit beta 3
COL1A2	Collagen type I alpha 2 chain
IGF1	Insulin like growth factor 1
COL1A1	Collagen type I alpha 1 chain
VTN	Vitronectin
FBN1	Fibrillin 1
LUM	Lumican
COL3A1	Collagen type III alpha 1 chain
SPARC	Secreted protein acidic and cysteine rich

pathway analysis for the significantly upregulated DEGs in ameloblastoma. It revealed that the major gene ontology terms and pathways were related to the extracellular matrix organization, collagen binding, cell adhesion and cell surface interactions. The Reactome pathway analysis showed the major pathways are associated with extracellular matrix organization, degradation of extracellular matrix, collagen synthesis, formation and degradation, integrin cell surface interactions and regulation of Insulin-like Growth Factor (IGF) transport and uptake by IGF-binding proteins.

Protein-protein interaction network and hub gene identification

The Protein-Protein Interaction (PPI) network was created in STRING for the significantly upregulated genes and visualized using Cytoscape. The resulting interaction network included 1276 nodes and 588 edges. The top 10 nodes from the three cytoHubba algorithms (MNC, Degree and Closeness) (Table 1) were used to identify the hub genes. The overlapping genes in the three algorithms (Fig. 1D) were considered as hub genes. These included fibronectin 1(FN1), collagen type I alpha1 chain (COL1A1), collagen type I alpha 2 chain (COL1A2), lumican (LUM), collagen type III alpha 1 chain (COL3A1), integrin subunit beta 3 (ITGB3) and insulin-like growth factor 1(IGF-1) (Fig. 1E; Table 1). Among these, FN1, COL1A1/COL1A2 and IGF-1 related to extracellular matrix organization, collagen binding, cell adhesion and cell surface interaction were selected for validation by immunohistochemistry using human ameloblastoma, mouse ameloblastoma xenograft and OKC tissues.

Validation of extracellular matrix protein expression by immunohistochemical analysis

The EPAMCs formed appreciable ameloblastoma tumor nodules within 4 weeks (Fig. 3) at time point the xenografts were harvested. Representative immunostained tissue sections showed that ameloblastoma stromal cells were immunoreactive to FN1, IGF-1 and COL 1 while the epithelial cells and epithelial islands were non-reactive (Fig. 4). Ameloblastoma xenograft and OKC presented similar immunoreactivity to both FN1 and IGF-1 but COL 1 reactivity was minimal to no reactivity (Fig. 4). Relative qualitative analysis of immunostaining intensities based on optical density measurements showed that FN1 demonstrated strongest staining intensity in both ameloblastoma and xenograft tissues unlike OKC (Fig. 5).

Discussion

Ameloblastoma and OKC are odontogenic pathological lesions associated with dental epithelium [25]. The present study accessed GEO database and analyzed publicly available GSE186489 gene expression data from ameloblastoma and OKC patients to further understand similarities and disparities between both locally invasive odontogenic lesions. We conducted bioinformatics analysis of ameloblastoma and OKC transcriptome and identified 1282 upregulated genes and 560 downregulated genes in ameloblastoma versus OKC. Furthermore, we assessed the DEGs in the GO, performed pathway analysis and used immunostaining to provide mechanistic insights into pathogenesis and growth characteristics of ameloblastoma.

Our analysis revealed that genes disparately upregulated in ameloblastoma are related to the extracellular matrix organization, degradation of extracellular matrix, collagen binding, collagen biosynthesis, collagen degradation, cell adhesion and cell surface interactions. We also identified the following seven hub genes (Table 1), FN1, COL1A1, COL1A2, LUM, COL3A1, ITGB3 and

Fig. 3 Representative mouse image showing appreciable ameloblastoma tumor nodules (black arrows) formed within 4 weeks by transplanted EPAMCs. The ruler adjacent to the mouse allows for comparison of the tumor size with the whole animal size

IGF-1 as upregulated in ameloblastoma using protein-protein interaction and network analysis. Similarly, FN1 and COL1A1 were also identified as hub genes in another study that analyzed two microarray datasets GSE132124 ($n=8$ ameloblastoma samples) and GSE38494 ($n=15$ ameloblastoma samples). However, ameloblastoma was compared to the normal tissue in this study [26]. These support numerous reports that dysregulation of the extracellular matrix plays modulatory roles in ameloblastoma invasion and progression. They also suggest that ameloblastoma interacts with the extracellular matrix and related proteins such as collagen, fibronectin, lumican and growth factors like IGF-1.

Tumor cell interaction with extracellular matrix proteins plays a major role in tumor progression and aggressiveness and collagen remodeling in the tumor stroma facilitates the local invasiveness of tumor cells [27, 28]. Additionally, extracellular matrix remodeling and altered growth factor signaling by cancer associated fibroblasts in the tumor microenvironment (TME) promote tumor cell proliferation, angiogenesis and invasiveness in numerous cancer types [29–31]. Reports on the interplay of extracellular matrix proteins and growth factors on the locally aggressive growth properties of ameloblastoma are still limited. In this study, we assessed expressions of FN1, COL I and IGF-1 in ameloblastoma, mouse ameloblastoma xenografts and OKC using immunohistochemistry to validate RNA sequencing data.

FN1 is one of the major extracellular matrix proteins involved in fundamental cellular processes such as cell

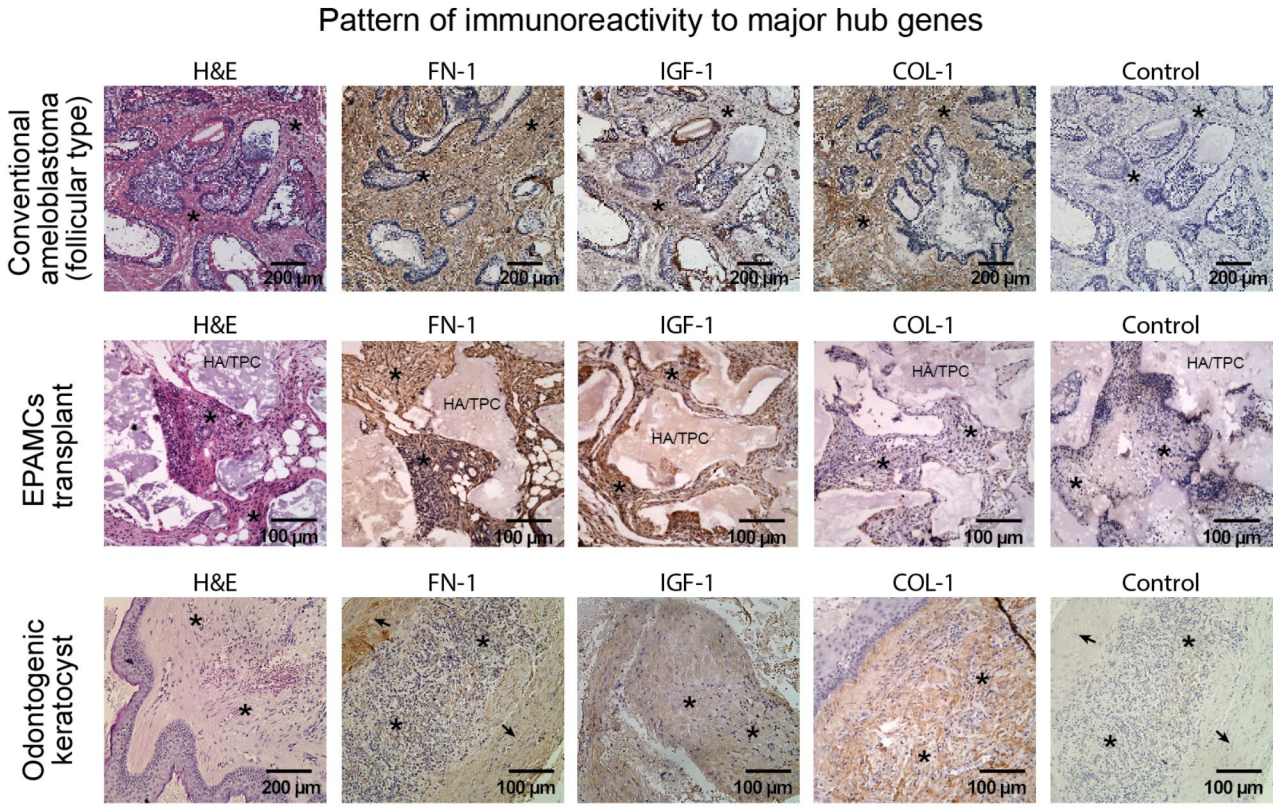

Fig. 4 Pattern of immunoreactivity to major hub genes. Immunohistochemical staining of conventional ameloblastoma (top panel), mouse ameloblastoma xenograft derived from EPAMCs also isolated from conventional ameloblastoma (middle panel) and OKC (lower panel). The stromal compartments (black star) of ameloblastoma and mouse ameloblastoma xenografts were strongly immunoreactive to FN1, IGF-1 and COL1 (top panel, columns 2,3 and 4). Similarly, stroma of mouse ameloblastoma xenograft (black star) was immunoreactive to FN1 and IGF-1 (middle panel, columns 2 and 3) but displayed minimal to no reactivity to COL I (middle panel, column 4). Similarly, the lower panel shows that stromal components (black star) of OKC immunoreacted with FN1, IGF-1 and COL 1 (lower panel, columns 2, 3 and 4). Additionally, OKC epithelial lining cells displayed (black arrows, column 2) immunoreactivity to FN-1. Comparative hematoxylin/eosin and negative antibody control tissue sections are shown in columns 1 and 5 respectively [Antibodies to FN1 = fibronectin 1; IGF-1 = insulin-like growth factor 1 and COL I = collagen 1. H&E = hematoxylin/eosin; control = non-immune serum; HA/TPC = hydroxyapatite/tricalcium phosphate carrier particles]

adhesion, migration, and wound healing [32]. There is increased expression of FN1 in various types of cancers including thyroid cancer and melanoma that are positive for BRAFV600E like ameloblastoma [27, 33–36]. FN1 promotes melanoma tumor proliferation and metastasis by regulating epithelial mesenchymal transition (EMT) and BRAFV600E tumor derived fibronectin regulates BRAF signaling pathway to promote invasion of melanoma cells [36, 37]. Previous studies showed abundant expression levels of FN1 in the stromal compartment of most types of ameloblastoma with characteristic medium to high expression levels near the epithelial mesenchymal interface [38, 39]. Our data not only align with these reports but also showed that high FN1 expression level was recapitulated in the mouse xenograft model of ameloblastoma formed by transplanted EPAMCs (Fig. 4). FN1 induces EMT in human breast cancer through ERK/MAPK pathway [40] and fibronectin fibrils regulate EMT induced by TGFβ in vitro [41]. It also promotes tumor progression in non-small cell lung cancer through integrin αvβ3/PI3K/AKT/SOX2 signaling pathway [33]. All these pathways have been associated directly or indirectly with ameloblastoma growth characteristics [1]. Interestingly, downregulation of FN1 in colorectal cancer was found to inhibit the carcinogenesis of colorectal cancer by suppressing tumor migration and proliferation [42], which makes a case for FN1 as a therapeutic target for ameloblastoma.

Collagen I (COL I) is a major component of the extracellular matrix and its abundance is associated with tumor cell proliferation and metastasis of many types of cancers [43, 44]. COL I is highly expressed in the stroma of plexiform, follicular and desmoplastic ameloblastoma [38, 45]. In our study, COL I expression was high in the stromal compartment of conventional follicular types of ameloblastoma that we assessed, but interestingly there was negative immunoreactivity in the EPAMC-induced mouse ameloblastoma xenograft and OKC (5). The

negative immunoreactivity in the xenograft could relate to the lower degree of invasiveness in the ameloblastoma xenograft due to partial loss of viable cells during the transplant procedure. While we found low COL-1 expression levels in OKC, another study that reported a high COL-1 expression in OKC normalized their results with normal oral mucosa tissues and not ameloblastoma only [46]. Transcriptomics analysis that showed upregulated collagen related genes such as COL1A1, COL3A1 in OKC were also compared to normal oral mucosa and not ameloblastoma [46]. Our observed higher expression levels of COL I in ameloblastoma is supported by tumoroid analysis in another study. It was reported that unlike OKC, COL I is required for progression and invasiveness of ameloblastoma based on extracellular matrix remodeling and altered collagen alignment within the tumor [47].

Transcriptomic analysis of AM-1 cells and ameloblastoma tissues revealed that extracellular matrix and EMT related proteins were upregulated in ameloblastoma tissue compared to AM-1 cells possibly due to the presence of stromal region in the ameloblastoma tissue [48]. To further understand this possible effect, AM-1 cells were cultured in matrigel and collagen gel to mimic the tumor stromal environment. The study reported that ECM remodeling was observed in the tumoroid cultured in collagen gel and not in the matrigel and increasing the type I collagen concentration also significantly increased the invasion distance of AM-1 cells [48]. Again, this showed that collagen rich matrix is essential for the aggressive growth and invasion of ameloblastoma [48]. High expression of COL I observed in colorectal cancer, another BRAFV600E-positive tumor was associated with stemness of cancer cells and metastasis mediated through integrin/PI3K/AKT/Snail signaling pathway [49]. COL I also promoted EMT through TGFβ in lung cancer cells [50]. COL I and FN1 co-promote aggressive phenotype in breast cancer cells and the activation of AKT and CDC42 signaling pathways via αvβ3 integrin resulted in growth and relapse of glioma tumor [28, 51]. Hence, the interplay of FN1, COL I and ITGB3 found to be highly upregulated in ameloblastoma relative to OKC may be a modulator of the tumor microenvironment and signaling pathways that enhance its locally aggressive growth properties.

Insulin like growth factors and their receptors are involved in human dental pulp stem cells proliferation and odontogenic differentiation through MAPK pathway. Similarly, IGF-1 interaction with bone morphogenetic proteins facilitates development of teeth, bone and cartilage. Along this line, IGF-1 was highly expressed in both ameloblastoma and calcifying odontogenic epithelial tumors [52]. We also found that both ameloblastoma and EPAMC mouse ameloblastoma xenograft were strongly positive for IGF-1. Considering higher IGF-1 gene expression levels in ameloblastoma relative to OKC (Fig. 5), IGF-1 could be a potential inducer of

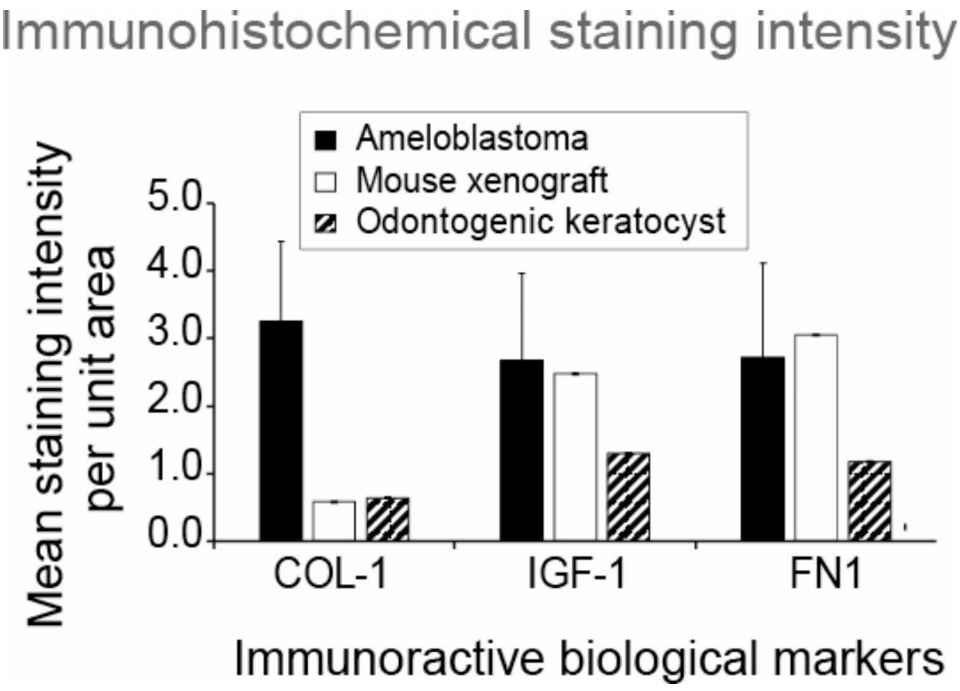

Fig. 5 Quantitative analysis of immunoreactivity to major hub genes. The bar graph shows average mean intensity per unit area of the optical density of four randomly selected regions of interest (ROI) normalized to its respective control tissues. Ameloblastoma was relatively the most immunoreactive to the FN1, IGF-1 and COL I (FN1 = fibronectin 1; IGF-1 = insulin-like growth factor 1 and COL I = collagen 1),

invasiveness and proliferation in concert with integrins as previously reported in cervical cancers [53].

In ameloblastoma, the native stromal architecture enhances tumor microenvironment and invasiveness compared to non-native stromal architecture [54]. Hence, the current study validates differentially upregulated expression of matrix proteins FN1, COL I and IGF-1 in ameloblastoma relative to OKC because all the three genes and related proteins were more highly expressed throughout the tumor stroma in ameloblastoma. We identified multiple differentially expressed genes between ameloblastoma and OKC. Additionally, our validation studies indicate that the higher expressions of extracellular matrix organizations genes COL 1 and FN-1 combined with higher IGF-1 expression (Fig. 5) could support an interplay of these differentially upregulated genes in ameloblastoma. Consequently, these could contribute to the much more locally-invasive growth characteristics of ameloblastoma relative to OKC.

This study has some limitations. First, the GSE186489 gene expression data from GEO database analyzed were obtained from a limited number of ameloblastoma and OKC patient samples. Second, available information on the patient samples was limited to identification of the tumors as primary tumors, so recurrent and metastasizing ameloblastomas were not included. Third, OKC mouse xenografts were not directly compared by immunohistochemistry with ameloblastoma xenografts. These direct comparisons are interesting studies to pursue in future. However, more functional studies that assess the interplay of FN1, COL 1 and IGF-1 in modulating ameloblastoma tumor microenvironment will further enhance our knowledge of ameloblastoma growth properties as well as the development of biomarkers and therapeutic targets for ameloblastoma.

Supplementary Information

The online version contains supplementary material available at https://doi.org/10.1186/s12903-024-04866-7.

Supplementary Material 1

Acknowledgements
We thank Dr. Abdul-Warith Akinshipo, Lagos University Teaching Hospital, Lagos Nigeria for providing the OKC tissue blocks.

Author contributions
PJ: Acquisition of data, analysis of data, drafting of article and critical revision of manuscript. AA: Design of study, acquisition of data, analysis of data, drafting of article and critical revision of manuscriptSOA: Conception and design of study, analysis of data, drafting of article and critical revision and final approval of manuscript.

Funding
The study was supported by grant R01CA259307 (awarded to S. O. A.) by the United States Department of Health and Human Services/National Institutes of Health, Bethesda, MD, USA and the Penn Global Research and Engagement Grant -Holman Africa Research and Engagement Fund, University of Pennsylvania, Philadelphia, PA, USA.

Data availability
The GSE186489 datasets analyzed during the current study are available in the Gene Expression Omnibus repository [https://www.ncbi.nlm.nih.gov/geo/query/acc.cgi?acc=GSE186489] Supplementary table of differentially expressed genes is provided.

Declarations

Ethics approval and consent to participate
Ameloblastoma tissues were collected from patients enrolled in Protocol 849,919. The Protocol and Waiver of Informed Consent were approved by University of Pennsylvania Office of Regulatory Affairs Institutional Review Board (IRB). Waiver of Informed Consent was approved. Mouse xenograft model of ameloblastoma performed under animal protocol (# 806165) approved by the University of Pennsylvania Institutional Animal Care and Use Committee (IACUC).

Consent for publication
Not applicable.

Competing interests
The authors declare no competing interests.

Author details
[1]Department of Oral Medicine, School of Dental Medicine, University of Pennsylvania, Philadelphia, PA, USA

Received: 10 February 2024 / Accepted: 5 September 2024
Published online: 13 September 2024

References

1. Effiom OA, Ogundana OM, Akinshipo AO, Akintoye SO. Ameloblastoma: current etiopathological concepts and management. Oral Dis. 2018;24(3):307–16.
2. Medina A, Velasco Martinez I, McIntyre B, Chandran R. Ameloblastoma: clinical presentation, multidisciplinary management and outcome. Case Rep Plast Surg Hand Surg. 2021;8(1):27–36.
3. Hendra FN, Van Cann EM, Helder MN, Ruslin M, de Visscher JG, Forouzanfar T, de Vet HCW. Global incidence and profile of ameloblastoma: a systematic review and meta-analysis. Oral Dis. 2020;26(1):12–21.
4. Brown NA, Betz BL. Ameloblastoma: a review of recent molecular pathogenetic discoveries. Biomark Cancer. 2015;7(Suppl 2):19–24.
5. Anbinselvam A, Akinshipo AO, Adisa AO, Effiom OA, Zhu X, Adebiyi KE, Arotiba GT, Akintoye SO. Comparison of diagnostic methods for detection of BRAFV600E mutation in ameloblastoma. J Oral Pathol Med. 2024;53(1):79–87.
6. AlMuzaini A, Boesze-Battaglia K, Alawi F, Akintoye SO. Hypoxia enhances basal autophagy of epithelial-derived ameloblastoma cells. Oral Dis. 2022;28(8):2175–84.
7. Sharp RC, Effiom OA, Dhingra A, Odukoya O, Olawuyi A, Arotiba GT, Boesze-Battaglia K, Akintoye SO. Enhanced basal autophagy supports ameloblastoma-derived cell survival and reactivation. Arch Oral Biol. 2019;98:61–7.
8. Board WCTE. Head and Neck Tumours. In: WHO classification of tumours series 5th edition. 9, 2022 edn. Lyon, France: International Agency for Research on Cancer; 2022.
9. Soluk-Tekkesin M. JM Wright 2022 The World Health Organization Classification of Odontogenic Lesions: a Summary of the changes of the (5th) Edition. Turk Patoloji Derg 2022;38()2:168–84.
10. Mishra P, Panda A, Bandyopadhyay A, Kumar H, Mohiddin G. Sonic hedgehog signalling pathway and ameloblastoma - A review. J Clin Diagn Res. 2015;9(11):ZE10–13.
11. Magliocca KR. Proceedings of the 2023 North American Society of Head and Neck Pathology Companion Meeting, New Orleans, LA, March 12, 2023: Odontogenic Tumors: Have We Achieved an Evidence-Based Classification. Head Neck Pathol 2023;17(2):313–324.
12. Li TJ. The odontogenic keratocyst: a cyst, or a cystic neoplasm? J Dent Res. 2011;90(2):133–42.

13. Jain KS, Bodhankar K, Desai RS, Bansal S, Shirsat P, Prasad P, Shah A. Absence of BRAFV600E immunohistochemical expression in sporadic odontogenic keratocyst, syndromic odontogenic keratocyst and orthokeratinized odontogenic cyst. J Oral Pathol Med. 2020;49(10):1061–7.
14. Zhang R, Yang Q, Qu J, Hong Y, Liu P, Li T. The BRAF p.V600E mutation is a common event in ameloblastomas but is absent in odontogenic keratocysts. Oral Surg Oral Med Oral Pathol Oral Radiol. 2020;129(3):229–35.
15. Cha YH, Cho ES, Kang HE, Ko J, Nam W, Kim HJ, Kim NH, Kim HS, Cha IH, Yook JI. Frequent oncogenic BRAF V600E mutation in odontogenic keratocyst. Oral Oncol. 2017;74:62–7.
16. Heikinheimo K, Kurppa KJ, Laiho A, Peltonen S, Berdal A, Bouattour A, Ruhin B, Caton J, Thesleff I, Leivo I, et al. Early dental epithelial transcription factors distinguish ameloblastoma from keratocystic odontogenic tumor. J Dent Res. 2015;94(1):101–11.
17. Xiong G, Xie N, Nie M, Ling R, Yun B, Xie J, Ren L, Huang Y, Wang W, Yi C, et al. Single-cell transcriptomics reveals cell atlas and identifies cycling tumor cells responsible for recurrence in ameloblastoma. Int J Oral Sci. 2024;16(1):21.
18. Graillon N, Akintoye SO, Iocca O, Kaleem A, Hajjar S, Imanguli M, Shanti RM. Current concepts in targeted therapies for benign tumors of the jaw - A review of the literature. J Craniomaxillofac Surg. 2023;51(10):591–6.
19. Ge SX, Son EW, Yao R. iDEP: an integrated web application for differential expression and pathway analysis of RNA-Seq data. BMC Bioinformatics. 2018;19(1):534.
20. Li H, Yang L, Hou Y, Zhang Y, Cui Y, Li X. Potential involvement of polycystins in the pathogenesis of ameloblastomas: analysis based on bioinformatics and immunohistochemistry. Arch Oral Biol. 2023;149:105662.
21. Ge SX, Jung D, Yao R. ShinyGO: a graphical gene-set enrichment tool for animals and plants. Bioinformatics. 2020;36(8):2628–9.
22. Fabregat A, Sidiropoulos K, Viteri G, Forner O, Marin-Garcia P, Arnau V, D'Eustachio P, Stein L, Hermjakob H. Reactome pathway analysis: a high-performance in-memory approach. BMC Bioinformatics. 2017;18(1):142.
23. Vered M, Wright JM. Update from the 5th Edition of the World Health Organization Classification of Head and Neck tumors: odontogenic and maxillofacial bone tumours. Head Neck Pathol. 2022;16(1):63–75.
24. Akinshipo AO, Effiom OA, Odukoya O, Akintoye SO. Consistency of color-deconvolution for analysis of image intensity of alpha smooth muscle actin-positive myofibroblasts in solid multicystic ameloblastomas. Biotech Histochem. 2020;95(6):411–7.
25. Bilodeau EA, Collins BM. Odontogenic cysts and Neoplasms. Surg Pathol Clin. 2017;10(1):177–222.
26. Zhang Z, Peng Y, Dang J, Liu X, Zhu D, Zhang Y, Shi Y, Fan H. Identification of key biomarkers related to epithelial-mesenchymal transition and immune infiltration in ameloblastoma using integrated bioinformatics analysis. Oral Dis. 2023;29(4):1657–67.
27. Li J, Chen C, Chen B, Guo T. High FN1 expression correlates with gastric cancer progression. Pathol Res Pract. 2022;239:154179.
28. Nolan J, Mahdi AF, Dunne CP, Kiely PA. Collagen and fibronectin promote an aggressive cancer phenotype in breast cancer cells but drive autonomous gene expression patterns. Gene. 2020;761:145024.
29. Zhi X, Lamperska K, Golusinski P, Schork NJ, Luczewski L, Golusinski W, Masternak MM. Expression levels of insulin-like growth factors 1 and 2 in head and neck squamous cell carcinoma. Growth Horm IGF Res. 2014;24(4):137–41.
30. Ferreira Mendes JM, de Faro Valverde L, Torres Andion Vidal M, Paredes BD, Coelho P, Allahdadi KJ, Coletta RD, Souza BSF, Rocha CAG. Effects of IGF-1 on Proliferation, Angiogenesis, Tumor Stem Cell Populations and Activation of AKT and Hedgehog Pathways in Oral Squamous Cell Carcinoma. Int J Mol Sci 2020;21(18).
31. Erdogan B, Webb DJ. Cancer-associated fibroblasts modulate growth factor signaling and extracellular matrix remodeling to regulate tumor metastasis. Biochem Soc Trans. 2017;45(1):229–36.
32. Hsiao CT, Cheng HW, Huang CM, Li HR, Ou MH, Huang JR, Khoo KH, Yu HW, Chen YQ, Wang YK, et al. Fibronectin in cell adhesion and migration via N-glycosylation. Oncotarget. 2017;8(41):70653–68.
33. Wu JL, Xu CF, Yang XH, Wang MS. Fibronectin promotes tumor progression through integrin alphavbeta3/PI3K/AKT/SOX2 signaling in non-small cell lung cancer. Heliyon. 2023;9(9):e20185.
34. Ramos Gde O, Bernardi L, Lauxen I, Sant'Ana Filho M, Horwitz AR, Lamers ML. Fibronectin modulates cell adhesion and signaling to promote single cell Migration of highly invasive oral squamous cell carcinoma. PLoS ONE. 2016;11(3):e0151338.
35. Sponziello M, Rosignolo F, Celano M, Maggisano V, Pecce V, De Rose RF, Lombardo GE, Durante C, Filetti S, Damante G, et al. Fibronectin-1 expression is increased in aggressive thyroid cancer and favors the migration and invasion of cancer cells. Mol Cell Endocrinol. 2016;431:123–32.
36. Gaggioli C, Robert G, Bertolotto C, Bailet O, Abbe P, Spadafora A, Bahadoran P, Ortonne JP, Baron V, Ballotti R, et al. Tumor-derived fibronectin is involved in melanoma cell invasion and regulated by V600E B-Raf signaling pathway. J Invest Dermatol. 2007;127(2):400–10.
37. Li B, Shen W, Peng H, Li Y, Chen F, Zheng L, Xu J, Jia L. Fibronectin 1 promotes melanoma proliferation and metastasis by inhibiting apoptosis and regulating EMT. Onco Targets Ther. 2019;12:3207–21.
38. de Medeiros AM, Nonaka CF, Galvao HC, de Souza LB, Freitas Rde A. Expression of extracellular matrix proteins in ameloblastomas and adenomatoid odontogenic tumors. Eur Arch Otorhinolaryngol. 2010;267(2):303–10.
39. Lapthanasupkul P, Poomsawat S, Chindasombatjaroen J. Investigation of basement membrane proteins in a case of granular cell ameloblastoma. Int J Oral Sci. 2012;4(1):45–9.
40. Park J, Schwarzbauer JE. Mammary epithelial cell interactions with fibronectin stimulate epithelial-mesenchymal transition. Oncogene. 2014;33(13):1649–57.
41. Griggs LA, Hassan NT, Malik RS, Griffin BP, Martinez BA, Elmore LW, Lemmon CA. Fibronectin fibrils regulate TGF-beta1-induced epithelial-mesenchymal transition. Matrix Biol. 2017;60–61:157–75.
42. Cai X, Liu C, Zhang TN, Zhu YW, Dong X, Xue P. Down-regulation of FN1 inhibits colorectal carcinogenesis by suppressing proliferation, migration, and invasion. J Cell Biochem. 2018;119(6):4717–28.
43. Jiang Y, Wang B, Li JK, Li SY, Niu RL, Fu NQ, Zheng JJ, Liu G, Wang ZL. Collagen fiber features and COL1A1: are they associated with elastic parameters in breast lesions, and can COL1A1 predict axillary lymph node metastasis? BMC Cancer. 2022;22(1):1004.
44. Li G, Jiang W, Kang Y, Yu X, Zhang C, Feng Y. High expression of collagen 1A2 promotes the proliferation and metastasis of esophageal cancer cells. Ann Transl Med. 2020;8(24):1672.
45. Vangansewinkel T, Driesen R, Agbaje J, Gervois P, Adisa A, Olusanya A, Arotiba J, Wolfs E, Lambrichts I, Politis C. Differential expression of fibroblast activation protein-alpha and lysyl oxidase in subtypes of ameloblastoma; 2023.
46. Zhong NN, Li SR, Man QW, Liu B. Identification of Immune Infiltration in Odontogenic Keratocyst by Integrated Bioinformatics Analysis. BMC Oral Health. 2023;23(1):454.
47. Li S, Lee DJ, Kim HY, Kim JY, Jung YS, Jung HS. Ameloblastoma modifies tumor microenvironment for enhancing invasiveness by altering collagen alignment. Histochem Cell Biol. 2022;158(6):595–602.
48. Li S, Lee DJ, Kim HY, Harada H, Jung YS, Jung HS. Transcriptomic Comparison Analysis between Ameloblastoma and AM-1 cell line. Int J Stem Cells. 2022;15(4):415–21.
49. Wu X, Cai J, Zuo Z, Li J. Collagen facilitates the colorectal cancer stemness and metastasis through an integrin/PI3K/AKT/Snail signaling pathway. Biomed Pharmacother. 2019;114:108708.
50. Shintani Y, Maeda M, Chaika N, Johnson KR, Wheelock MJ. Collagen I promotes epithelial-to-mesenchymal transition in lung cancer cells via transforming growth factor-beta signaling. Am J Respir Cell Mol Biol. 2008;38(1):95–104.
51. Zhong C, Tao B, Tang F, Yang X, Peng T, You J, Xia K, Xia X, Chen L, Peng L. Remodeling cancer stemness by collagen/fibronectin via the AKT and CDC42 signaling pathway crosstalk in glioma. Theranostics. 2021;11(4):1991–2005.
52. Alkutaifan H, Alnour A, Almohareb M. Immunohistochemical study of insulin-like growth factor 1 in calcifying epithelial odontogenic tumor and ameloblastoma: experimental research. Ann Med Surg (Lond). 2023;85(4):812–9.
53. Shen MR, Hsu YM, Hsu KF, Chen YF, Tang MJ, Chou CY. Insulin-like growth factor 1 is a potent stimulator of cervical cancer cell invasiveness and proliferation that is modulated by alphavbeta3 integrin signaling. Carcinogenesis. 2006;27(5):962–71.
54. Bakkalci D, Zubir AZA, Khurram SA, Pape J, Heikinheimo K, Fedele S, Cheema U. Modelling stromal compartments to recapitulate the ameloblastoma tumour microenvironment. Matrix Biol Plus. 2022;16:100125.

Publisher's note